

Design and research of intelligent wiper for automobile

Yuping Chen

Jiangsu Wuxi Institute of Transportations & Communications

WuXi, China

e-mail:307269161@QQ.com

Abstract—based on the principle of light intensity change puts forward a new type of car infrared rain sensor design, by infrared rain sensor perception rainfall size, make the wiper intelligently work state in high or low speed, to replace the traditional mechanical structure of the wiper. Based on the single-chip microcomputer, the software and hardware design of raindrop sensor is completed. The design conforms to the principle of humanization and can deal with various unexpected situations, which has a good application prospect.

Keywords- raindrop sensor; Single chip microcomputer; wiper

1 Introduction

According to statistics, rainy day driving with 7% of the world's accident was caused by the driver manual wiper, so now more installed in car rain sensors in order to increase the initiative and passive safety of driving. As the information source of automotive electronic control system, automobile sensor is the key component of automotive electronic control system and one of the core contents of automotive electronic technology research. In the research of automobile wiper, intelligent raindrop sensor naturally becomes an important part of intelligent wiper system. Intelligent sensor is high-grade sensor with intelligent functions, with functions of detection, information processing, automatic error compensation, high precision, large coverage range, good stability, large output signal anti-jamming, high signal-to-noise ratio, the transmission performance is good, the signal can be transmitted over a long distance, sometimes with a self-check function. The adoption of automatic wiper control system based on raindrop induction can save the driver from the trouble of manual operation of wiper and effectively improve the safety of driving in rainy days.

2 Hardware composition and module introduction

The raindrop sensor of wiper consists of two modules, transmitting module and receiving module. The main chip in the motor part is the four-bus buffer gate 74LS125.

2.1 Transmitting module

Launch module is its main function is to provide enough radiation flux for receiving module, the design of light source as the infrared, so the launch module by eight infrared emitter and a 555 timer and resistance capacitance component composition. The eight infrared transmitters are four in a group, two in parallel, driven by a 555 timer.

(1) transmitting tube: the transmitting tube adopts SFH421 produced by Siemens as the light source. The peak wavelength is 880 nm, and the bandwidth $\lambda < 80$ nm. It has high linearity, high reliability and high pulse processing capability. Four groups and two groups are used in parallel, driven by a 555 timer and emitting infrared light with a frequency of 38 kHz. Working at 38 kHz frequency, this method can reduce the power consumption of transmitting circuit.

(2) the multivibrator composed of 555 timer: at the heart of the transmitter is oscillator, multivibrator is a kind of self-excited oscillation circuit, the circuit is in after turning on the power supply without external trigger signal can produce a certain frequency and amplitude of rectangular or square wave pulse. Can be made of integrated circuit of inverter, nand gate, no steady state circuit, 555 timer, etc. Among them the 555 timer of oscillation of the system is easy to start up, its output power is larger, the commonly used of the launch system, its principle diagram is shown in figure 1:

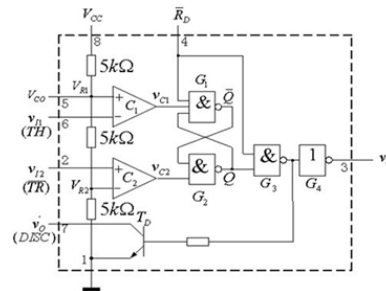


Figure 1 555 principle diagram of timer

In figure 1, the comparative voltages of C_1 and C_2 are $\frac{2}{3} V_{cc}$ and $\frac{1}{3} V_{cc}$ respectively. After turning on the power supply, the capacitance v_c is charging, when up v_c , $\frac{2}{3} v_{c c}$, triggers are reset, at the same time discharge BJT T conduction, the v as the low level, discharge, capacitance C by R and T decreased v_0 . When v_c drops to $\frac{1}{3} v_{c c}$, the trigger is set again, and v_0 is flipped to a high level. Capacitor C discharge time required is:

$$t_{PL} = (R_2 C \ln 2) \approx 0.7 R_2 C \quad (1)$$

When the discharge of C ends, T stops. $v_{c c}$ will charge the capacitor C through R_1 and R_2 . The time required for

v_c to rise from $\frac{1}{3}v_{c c}$ to $\frac{2}{3}v_{c c}$ is:

$$t_{PH} = (R_1 + R_2)C \ln 2 \approx 0.7(R_1 + R_2)C \quad (2)$$

When v_c goes up to $\frac{2}{3}v_{c c}$, the trigger flipped again, so

the cycle, get on the output side on a periodic square wave, the frequency is:

$$f = \frac{1}{t_{PL} + t_{PH}} \approx \frac{1.43}{(R_1 + 2R_2)C} \quad (3)$$

In this paper, we design the launch of a module is composed of 555 timer multivibrator, the values of R_1 , R_2 and C are calculated by equations (1), (2) and (3), the 555 circuit generates a pulse wave with a frequency of 38 kHz, which drives the infrared transmitter to operate at 38 kHz. Due to the high sensitivity of the comparator within 555 and the use of differential circuit, its oscillation frequency is little affected by voltage and temperature changes. Therefore, the change of power voltage has negligible effect on the transmitting frequency. But the impact on the infrared emission intensity of is not allow to ignore, must adopt measures to improve the stability of emission intensity, method is to adopt constant current source technology or narrow pulse emission measures, can make the infrared radiation intensity remains unchanged. The constant current source technology is adopted in this design.

2.2 Receiving module

the receiving module consists of an infrared receiving tube, a band pass filter, a frequency divider and a 51 microcontroller.

(1) infrared receiving tube, Siemens SFH320, NPN silicon photoelectric triode. The peak wavelength is 880 nm, which is characterized by high linearity and high reliability. After changing the received infrared ray pulse signal into an electrical pulse signal, it is fed into the bandpass filter.

(2) band-pass filter, which only allows the signal in a certain band to pass, but blocks the signal outside this band. It is often used in anti-interference equipment to receive effective signals within a certain frequency band and eliminate interference and noise in high frequency band and low frequency band. A band pass filter circuit can be obtained by connecting a low pass filter with a high pass filter. The schematic diagram is shown in figure 2.

In figure 2, the passband cutoff frequency of the low-pass filter is f^2 , that is, the low-pass filter only allows the signal of $f < f^2$ to pass through, the pass band cutoff frequency of the high pass filter is f^1 , that is, it only allows the signal of $f > f^1$ to pass through. Now, when the

two are connected in series, and $f^2 > f^1$, its passband is the covering part of the above two frequency bands, that is,

$f^2 - f^1$, and becomes a bandpass filter. The resistance R and capacitance C at the input end form a low power circuit, while the other capacitance C and resistance R form a high pass circuit, which are connected in series to the same phase input end of the integrated operational amplifier.

For the sake of convenience of estimation, $R_2 = 2R$ and $R_3 = R$ are set as, at this point, the voltage amplification factor of the bandpass filter can be obtained:

$$A_u = \frac{A_{uo}}{(3 + A_{uo}) + j(\frac{f}{f_0} - \frac{f_0}{f})} = \frac{A_{up}}{1 + jq(\frac{f}{f_0} - \frac{f_0}{f})} \quad (4)$$

In this design, the center frequency is 38kHz and the bandwidth is 100Hz, so Q is 380. The capacity of C is not easily exceeded $1\mu F$. Because the capacitors with large capacity are large in volume and high in price, they should be avoided as much as possible. According to equation $C = 0.1\mu F$, $1K\Omega < R < 1M\Omega$ and according to the following formula:

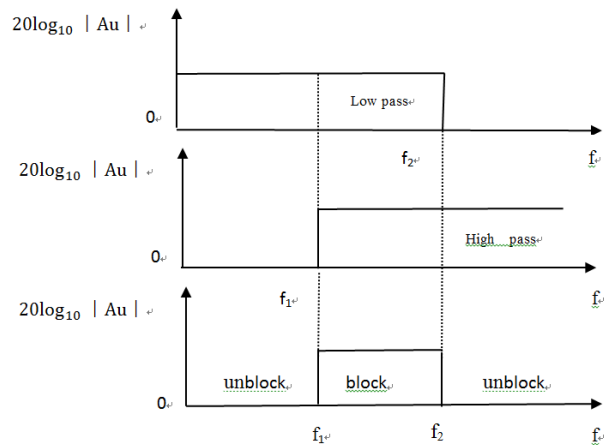
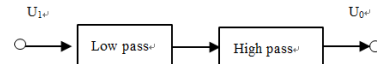
$$f_0 = \frac{1}{2\pi RC} = \frac{1}{2\pi R \times 0.1 \times 10^{-6}} = 38KHz \quad (5)$$

Calculate $R = 41.9\Omega$. And then we're going to solve for R_1 and R_f based on Q, when $f = f_0$, $Q = \frac{1}{3 - A_{uo}} = 380$,

so $A_{uo} = 2.997$, According to the relationship with A_{uo} , R_1 , R_f , integrated op-amp symmetry conditions of two input resistance, available:

$$1 + \frac{R_f}{R_1} = A_{uo} = 2.997, R_1 // R_f = R + R + R = 3R, \quad (6)$$

Solution: $R_1 = 188.7\Omega, R_f = 376.8\Omega$



3 Software and hardware design of intelligent wiper

3.1 Structure block diagram of intelligent wiper

The intelligent wiper system consists of single chip microcomputer, dc motor, raindrop sensor and wiper. The system structure diagram of the intelligent wiper is shown in figure 3.

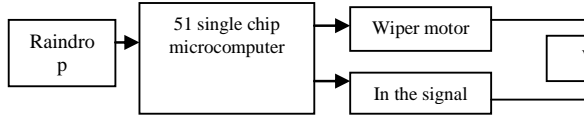


Figure 3 Smart wiper system structure diagram

3.2 hardware design of raindrop sensor

The raindrop sensor part, which consists of a 555 timer thanks to the oscillator, drives the infrared transmitter tube, which is then received by the receiver tube, thus forming a photoelectric sensor. The signal of the photoelectric sensor is limited to about 38KHZ by the band pass filter, and then 128 minutes by the frequency divider, so that the pulse signal becomes the order of milliseconds. The hardware diagram of such composition is shown in figure 4:

(1) hardware design of motor control

P0.0, P0.1, P0.3 and P0.4 of the P0 port of 80c51 microcontroller are respectively controlled by four photoelectric isolators and four high-power field effect switching tubes IRF640 through four bus buffer gate 74LS125 and reverse drive 74LS04. Below illustrates the control process of the circuit of A motor, when the microcontroller via P0 interface output 12 h control model, because the three states in latch 74LS125 1 door is open, so optoelectronic isolator LEI conduction and shine light activated triode output for the high level, thus making high power field effect switch tube IRF640 (v1) conduction. Similarly, tristate gate 4 in 74LS125 outputs a high level, so the photoelectric isolator LEI glows and directs, thereby enabling v4 to pass. And similarly analytically, v2 and v3 are off. Therefore, the current flows from left to right through the dc motor, making the motor turn forward. When the output of P0 interface is 09H, the tri-state gate 2,3 in the latch 74LS125 opens, allowing v2 and v3 to be connected, v1 and v4 to be switched off, and the current flows through the motor from right to left, causing the motor to reverse. SA0 is the left position switch of the motor. When SA0 is set to 1, the forward code is output. SA1 is the right position switch of the motor. When SA1 is set to one, the reverse code is output. The motor reset end is the left position switch of each motor.

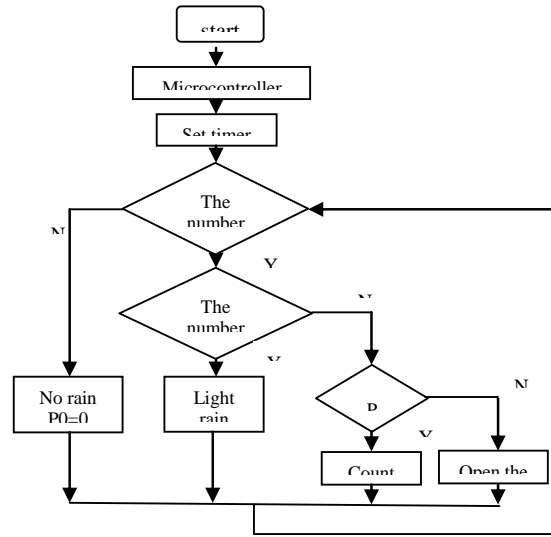


Figure 4 Flow chart of raindrop sensor

3.3 Software design of raindrop sensor

Because the center of the pulse frequency is 38 KHZ, approximately 300HZ, after 128 points frequency cycle is 3ms, so the timing for selected 60ms, in this time period can receive up to 20 pulse, resulting in the pulse of the distribution of many of the great rain, the resulting rain sensor flow chart shown in figure 5, 60ms timer flow diagram as shown in figure 5:

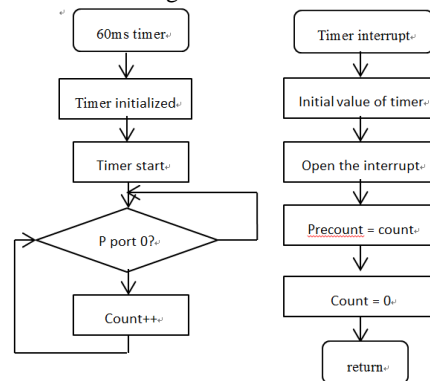


Figure 5 60ms timer flow chart

3.4 Main program flow chart design of intelligent wiper

In the intelligent wiper system, there are many nonlinear factors that affect the synchronization of wiper. In this way, we need human experience to adjust the duty ratio of PWM signal to make two wipers swing synchronously. Therefore, applying the fuzzy control technology to the synchronous control of wiper can make

the system have good control effect. The main program flow diagram of the intelligent wiper is shown in figure 6:

4. The conclusion

The raindrop sensor has completed hardware and software testing and is installed on the side of the driver's cab on the windscreen glass. By changing the amount of rainfall, the wiper can work automatically at low or high speed. The experimental results show that the intelligent wiper system is sensitive, the output signal delay is negligible and the performance is stable.

Reference

- [1] wang yanbo, design and implementation of automatic inductive wiper controller based on single-chip microcomputer, journal of Harbin university of technology [J],2009,14
- [2] sun jie automobile wiper control system design [J]- charming China 2010(26)
- [3] zhao yan. Zhang chungjing. Research on automobile wiper system based on fuzzy PID controller [J]- manufacturing automation 2010,32(2)
- [4] han li, wang zheng. 2010 Volkswagen beetle wiper won't work [J]. Automobile maintenance technician. 2018(03)
- [5] zhu mingjie. Use and maintenance of wiper [J]. Agricultural equipment technology. 2014(03)
- [6] nie yongtao, li yanfang, han zhiyin, Chen shao-zhi. Daily maintenance and repair of automobile wiper [J]. Automotive engineer. 2014(09)
- [7] village sister. Maintenance skills of automobile wiper [J]. Transportation and transportation. 2014(05)
- [8] clean heart. Wiper: wind and rain will accompany you to safety [J]. Road traffic management. 2013(08)
- [9] liu zheng, zeng lei. Design and application of new wiper [J]. Enterprise technology development. 2012(Z1)
- [10] zhou Yang. BMW 523Li wiper malfunction [J]. Car maintenance technician. 2010(12)
- [11] Shadow. Use of automobile windshield wiper and buy rainwater, please turn aside [J]. Contemporary automobile. 2010(01)
- [12] tong jianfeng. Proper use and maintenance of wiper [J]. Transportation and transportation. 2008(06)
- [13] zhou sudong, rong yu, fu kebao, ding zusheng. Analysis on rain scraper [J]. Agricultural machinery. 2007(04) [1] song kai, Yang heli. Design of intelligent wiper for automobiles [J]. Hebei agricultural machinery. 2016(10)
- [14] zhao haijun, wang Yang. A distributed sensor positioning algorithm based on multidimensional scaling [J]. Journal of jilin normal university (natural science edition). 2016(03)
- [15] huang qike, ma youliang, Chen xiaobing, cui ting. Design of intelligent wiper control system [J]. Road and steam transportation. 2014(01)
- [16] Chen yuping. Design and research of automobile intelligent wiper based on single-chip microcomputer [J]. Digital technology and application. 2013(02)
- [17] wang Ming, wu bingjin. Research on intelligent wiper control system based on CAN bus [J]. Journal of xihua university (natural science edition). 2012(04)
- [18] ren deqiang, wu qirong, gong min. Special control chip for intelligent wiper [J]. Electronics and packaging. 2011(10)
- [19] sun meidong, hu renjie, ma zhiyong. Intelligent control system of vehicle wiper [J]. Electrical and electrical engineering. 2009(12)
- [20] Chen hongchuan, su hu, Yang bin. Realization of windscreen rainy day effects in driving simulation [J]. Modern computer. 2013(13)